SAND--84-1741C
CONF-850706--

TIME-RESOLVED SPECTROSCOPIC STUDIES OF DETONATING HETEROGENEOUS EXPLOSIVES

Wayne M. Trott and Anita M. Renlund
Sandia National Laboratories
Albuquerque, New Mexico 87185

SAND--84-1741C

DE85 009760

Abstract

Emission spectroscopy and pulsed-laser-excited Raman scattering methods have been applied to the study of detonating heterogeneous explosives, including PETN, HMX and HNS. Time-resolved spectra of emission from detonating HNS show the evolution of features due to electronically-excited radical species. For HNS, the CN(B-X) system near 388 nm has been studied at a wavelength resolution of 0.5 A. Boltzmann vibrational temperatures have been calculated by comparing the experimental data with computer-simulated spectra. These temperatures are consistent with the expected trend of detonation temperature as a function of charge density. Using 532-nm laser excitation, single-pulse Raman scattering measurements have been made at the free surface of detonating HMX and PETN samples. Monotonic attenuation of Raman scattering intensity over a 100-ns interval is observed after detonation front arrival at the free surface. Depletion of the Raman signal occurs prior to significant loss of the scattered laser light. The significance of the Raman measurements as a possible probe of reaction zone length in detonating explosives is discussed.

This work was performed at Sandia National Laboratories, Albuquerque, NM, supported by the U. S. Department of Energy under contract number DE-AC04-76DP00789.

DISCLAIMER

DISCLAIMER

I. INTRODUCTION

A predictive understanding of the initiation and sustained detonation of heterogeneous (i. e., porous, granular) explosives requires characterization of both the mechanical response of the material and the chemical reaction mechanisms that control the rate at which the explosive is consumed. Real-time spectroscopic techniques offer considerable potential for providing much needed information on the important microscopic physical and chemical processes in such systems via in situ measurements of reaction intermediates, rates and temperatures. In this paper, we discuss the application of emission spectroscopy and pulsed-laser-excited Raman scattering methods to the study of detonating high explosives (HEs) including pentaerythritol tetranitrate (PETN), 1,3,5,7-tetranitro-1,3,5,7-tetraazacyclooctane (HMX) and 2,4,6,2',4',6'-hexanitrostilbene (HNS). Both techniques provide good temporal and spatial resolution and are applicable to pressed polycrystalline samples of many widely used HEs. In time-resolved emission studies, we have observed several electronically-excited transient species including CN^*, CH^*, $C_2{}^*$ and probably $NO_2{}^*$. Results of high-resolution studies of CN(B-X) emission in detonating HNS have been used to calculate vibrational temperatures as a function of initial charge density. We have shown that single-pulse Raman scattering measurements can be made in the severe environment of a detonation and have monitored the attenuation of the Raman signal from PETN as a function of time after detonation-wave arrival at the free surface. These results are compared to previous estimates of reaction time in an unperturbed, steady-state detonation.

II. EXPERIMENTAL

The explosive device used for all emission and Raman measurements consisted of a pressed pellet of pure HE initiated by an exploding bridgewire detonator (Reynolds Industries, RP-2). The pellet was affixed to the detonator output face using a thin layer of fast setting epoxy. The explosive assembly was mechanically held in a fixture providing for linear and angular alignment and all measurements were performed with the assembly confined in an evacuated chamber to avoid complications due to air. The detonator was connected to a 2.5-kV fireset using high-voltage vacuum feedthroughs. The specified detonator function time at this operating voltage is 1.8 μs with a standard deviation of less than 25 ns. The diameter of the HE pellet (6.4 mm) was roughly twice that of the detonator output face. The relatively small size of this configuration permitted reasonably frequent measurements with modest material consumption and minimal damage to the optical components mounted on the test chamber; however, the non-planar output of the device introduced some difficulty in data interpretation as discussed below. Samples of the various HEs were prepared by pressing approximately 100 mg of the loose powder. Densities of the pressed HMX and PETN were 1.87 and 1.69 g cm^{-3}, respectively. For HNS, material pressed to four different densities were used: ρ_o = 1.70, 1.65, 1.56 and 1.50 g cm^{-3}.

Temporal and spatial characteristics of the detonation light were examined using fast-framing photography. An Imacon 675

camera (Hadland Photonics Ltd., S-20 response) was used to obtain images of the detonating pellets at a framing rate of 7.5×10^7 s^{-1}. The camera monitor pulse (nearly coincident with the first frame) was recorded on each shot for comparison with the temporal profile of emission intensity as determined by either a photomultiplier or biplanar phototube. The framing records were obtained on Polaroid Type 47 film. The images were then digitized and contrast enhanced using a COMTAL "Vision One/20" image processing system.

In studies of spectrally resolved emission, light from the front face of the exploding pellet was imaged onto the slit of a spectrometer (Jarrell-Ash 1/3 m or Spex 0.85 m). The dispersed spectrum of near-uv and visible emission was viewed by a gatable intensified diode array coupled to an optical multichannel analyzer (Tracor Northern) allowing temporal resolution of <20 ns. Timing of the detector gate pulse relative to the firing pulse was varied with digital delay generators. For studies of temporally resolved spectra, signals from the detector gate and from a photomultiplier tube viewing the total emitted light were displayed together on an oscilloscope to establish the exact time interval over which the spectrum was obtained.

Detailed discussions of the experimental design for the single-pulse Raman scattering studies have been presented elsewhere.[1,2] A schematic of the experimental arrangement is given in Fig. 1. Briefly, the 532-nm output of a frequency-

doubled, pulsed Nd:YAG laser (~10 ns FWHM) was mildly focused to a 1-mm-diameter circular spot at the center of the free surface of the explosive pellet. Laser energy reaching the sample was controlled by varying the time delay to the Q-switch. The frequency-shifted radiation scattered from the sample was imaged onto a spectrometer and viewed with the intensified diode array and optical multichannel analyzer. A <100-ns-wide gate to the detector avoided signal loss due to timing jitter and provided some discrimination against the detonation emission. Digital delay generators were used to set the probe laser and detection system gate in relation to the fireset trigger pulse.

III. RESULTS AND DISCUSSION

A. Fast-Framing Photography

The emission phenomena observed in fast-framing photographic records of detonating HMX and HNS are generally consistent with the results of previous studies of detonation light.[3,4] Most of these phenomena are illustrated by the sequential images of a detonating HNS pellet displayed in Fig. 2. The first frame in this sequence shows a small bright spot of light corresponding to the emergence of the detonation wave at the center of the pellet surface. The rapidly expanding "ring" of bright emission seen in the next eight frames reveals the two-dimensional character of the detonation wave front in this device. This "ring" actually contains fine, granular structure which can be clearly seen in the images near the end of the sequence. The rapid quenching of

the bright emission is especially evident in Frame 2 where the region surrounding the center of the pellet surface is relatively dark compared to the same region in Frame 1. From the width of the emission ring, we estimate the duration of emission at any point on the surface to be on the order of the single frame exposure time; i. e., 3 ns or less.

A weaker, diffuse glow precedes the emergence of the detonation wave at the surface. This phenomenon is barely discernible at the outer edges of the bright emission in Frames 1-3 of Fig. 2 and was much more obvious in the case of detonating HMX. We attribute the diffuse glow to so-called "shine through"; i. e., light scattered from inside the pressed sample. The intensity of neither the bright ring nor the diffuse glow is much affected by pressure of surrounding atmosphere over the range 0.01 - 1 Torr. In contrast, after the detonation wave reaches the outer rim of the pellet surface, we observe emission (primarily in the form of a rapidly expanding ring of light) whose intensity is markedly dependent on the chamber pressure. The function of the surrounding atmosphere in production of this effect has been discussed previously. [4] At pressures below 50 mTorr, the observed "afterglow" intensity is approximately two orders of magnitude less than that of the bright emission coinciding with detonation front arrival at the surface of the sample. Accordingly, this phenomenon is not apparent in the late frames of Fig. 2 due to limited film contrast.

The various effects seen with fast-framing photography contribute to the observed temporal profile of emission intensity. In general, photomultiplier traces of the emission display (in order): (1) a slow-rising leading edge corresponding to increasing "shine through" as the detonation front approaches the free surface, (2) a rapid rise in signal intensity as the detonation wave front emerges from the end of the sample, (3) a plateau of high intensity due to the two-dimensional nature of the detonation front and (4) a rapid fall-off in signal as the detonation front reaches the outer rim of the material (see Section IIIC.) The photographic records are also very useful in the interpretation of our time-resolved emission spectra and provide an important measure of the non-planarity of the detonation front and its effect on our Raman scattering data.

B. Emission Spectroscopy

Figures 3-5 show spectra of emission from detonating HNS obtained at three different times relative to the arrival of the detonation wave at the free surface of the pellet. The spectra are corrected for the wavelength-dependent response of the spectrometer and detection system. In each case, emission was collected for a 30-ns interval to acquire sufficient signal. At the earliest time, which corresponds to primarily the "shine through" region and also to the initial break-out of the detonation (cf. Frame 1 in Fig. 2) the main feature of the emission is a broad unstructured band with an apparent cutoff

near 400 nm. We show calculated relative optical emission profiles for graybody sources at two temperatures together with the spectrum in Fig. 3. While there may be an underlying component of the emission due to graybody emission, it is clear that the shape of this broad band is not that of graybody radiation. Instead, this emission is consistent with NO_2(A-X) emission which is known to cut off at 398 nm due to predissociation of the NO_2.[5] A much smaller band in the 380-390 nm region is due to CN(B-X) emission. Figure 4 shows the spectrum obtained during the high-intensity emission corresponding to Frames 4-6 of Fig. 2. The most prominent feature is due to CN(B-X) emission. Approximately 100 ns later, we obtained the spectrum shown in Fig. 5 where products such as C_2(d) are also observed in emission. The presence of C_2(d-a) emission in the earlier spectra is not observed because of the intense broadband emission in the same spectral region. We have performed similar experiments with HMX. Again, the early emission appears to be primarily NO_2(A-X). Late-time emission, however, shows only weak discrete features of the electronically excited radical species and the spectrum is dominated by a broadband continuum different from the early emission. In general, the intensity of discrete emission appears to correlate in a reciprocal fashion with the degree to which the explosive is oxygen balanced, i. e., HNS > HMX > PETN.

In previous experiments, we have noted that the vibronic structure of the CN(B-X) and C_2(d-a) bands observed from

detonating HEs can be used to infer Boltzmann vibrational temperatures. [6] We have now extended these studies to higher spectral resolution to observe the effect of the initial charge density on the temperature of the CN(B). To obtain higher resolution, we sacrifice the temporal resolution of the previous spectra. Instead, we integrate the emission over 300 ns which includes all the emission except some of the weak "afterglow". Figures 6 and 7 show spectra in the CN(B-X) spectral region from detonating samples of HNS pressed to initial densities of 1.70 and 1.50 g cm^{-3}, respectively. These are typical of the resolution (~0.5 Å) and signal-to-noise ratio we are now able to achieve on a single shot. The most apparent difference between the two spectra is the smaller ratio of intensity in the (1,1) and (2,2) bands relative to the (0,0) band in the emission from detonating HNS pressed to the higher density (Fig. 6). To establish the vibrational temperature of the CN(B) in these two experiments, several CN(B-X) spectra were generated by computer simulation at temperatures between 3500 and 7500 K. To calculate these spectra, we assume equilibration of the vibrational and rotational degrees of freedom which allows relative populations in the rovibrational states of CN(B) to be described by a Boltzmann distribution at a single temperature. Published values of spectroscopic constants [7] and Franck-Condon factors [8] were used to calculate individual transition intensities as a function of the Boltzmann population distributions.[6] The spectra were then simulated using a Gaussian slit function appropriate for the resolution of the present experiments. The simulated spectra

were compared to the data to obtain a best fit, and are shown by the open circles in Figs. 6 and 7. These fits establish the temperatures of the emitting CN(B) at 5000±200 K and 6500±400K from detonating HNS at the high and low densities, respectively. Data from HNS pressed to two intermediate densities gave temperatures between these two values, following a trend of increasing temperature with decreasing initial charge density. While the agreement between the simulated spectra and the data is generally good, the simulated spectra fail to reproduce the width on the short-wavelength side of the bandheads for emission from the detonating low-density HNS (cf. Fig. 7). This may indicate incomplete equilibration of the rotational and vibrational modes of the emitting CN.

Our results show that emission spectroscopy at sufficiently high resolution provides a spectroscopic "thermometer" which may correlate with detonation temperature. The trend of detonation temperature, as calculated by equation-of-state models, with initial charge density is the same as we observe in our CN(B-X) measurements.[9] We note, however, that our measured temperatures are generally ~1000 K higher than results of most modelling calculations.[9]

C. Single-pulse Raman Scattering

Recently, there has been considerable interest in spontaneous and coherent Raman scattering techniques as diagnostic probes for determining the microscopic phenomenology of shock-induced

chemical reactions.[10] Spontaneous Raman spectroscopy has been used in several studies of detonating liquid and monocrystalline explosives. [11-14]] We have shown [1,2] that excellent single-pulse spontaneous Raman spectra can be obtained from many unshocked heterogeneous explosive samples and that Raman scattering measurements can be made in the severe environment of detonating PETN. Here, we utilize recent Raman scattering measurements from detonating HMX as well as the fast-framing photography data described in Section IIIA to expand our previous discussion [1] of Raman scattering from detonating heterogeneous explosives.

Our PETN results are reproduced in Figs. 8 and 9. Figure 8 compares the single-pulse Raman spectrum (800-1500 cm^{-1} range) of unshocked PETN with that obtained from a detonating sample at a time delay of 450 ns from the nominal RP-2 detonator function time, t_o. We observe remarkably similar positions of the Raman lines in the unshocked and detonating material; however, the significant attenuation of the Raman lines and simultaneous appearance of strong background emission are evidence that the detonation front has reached the free surface of the pellet. Under sustained compression at detonation pressures, substantial shifts in the molecular vibrational frequencies might be expected, but the complex interaction of the detonation wave front with the PETN/vacuum interface may preclude observation of such shifts. We also note that previously observed shock-induced frequency shifts in PETN single crystals have been much smaller

than those seen in static compression studies.[14,15] In Fig. 9, the measured attenuation of the strongest Raman line (the 1296 cm^{-1} line associated with the symmetric NO_2 stretching mode [16,17]) is shown as a function of time delay from t_o. The same figure also displays a trace of the observed emission intensity versus time delay from t_o. Depletion of the parent molecule Raman signal occurs over a 100-ns interval.

The observed interval for attenuation of the PETN Raman scattering intensity may reflect the chemical reaction rate for the parent species in this system. Alternative interpretations of this phenomenon include the following: (1) the Raman signal attenuation arises from a fairly large probe depth, (2) the two-dimensional nature of the detonation front is responsible for the observed interval, and (3) the Raman signal loss simply reflects a reduced surface area for scattering or increased optical absorption at the pellet surface. The nonzero probe depth and nonideal detonation front certainly contribute to the apparent depletion time by permitting the simultaneous observation of unshocked and shocked material as the detonation wave front nears the free surface; however the available data suggest that these are of only minor importance. Figure 8 shows that the onset of the Raman signal depletion coincides with a sharp rise in the emission intensity. As mentioned in Section IIIA, the rapid rise in the emission signal also coincides with the emergence of the detonation wave from the end of the pellet. Very little attenuation of the Raman scattering intensity occurs prior to

this event (cf. Fig. 8). Hence, we infer that the probe depth is actually quite small. Direct evidence concerning the possible effect of the non-planar detonation front is provided by the first two frames in Fig. 2. At Frame 2, we see that the detonation front has already emerged from the pellet over a surface area larger than the 1-mm-diameter probe laser spot. Frame 1, on the other hand, shows emission corresponding to the initial arrival of the detonation front at the center of the free surface. From these images, we estimate that the resulting temporal contribution to the observed interval for Raman signal depletion can be no more than the fast-framing camera interframe time; i. e., 15 ns or less.

To address the third alternative interpretation mentioned above, we have examined the Raman signal loss in relation to the intensity of scattered 532-nm light for unshocked and detonating samples. Typical results for HMX are given in Figs. 10 and 11. The data in each figure were obtained using a single 532-nm laser pulse. The scattered laser light was attenuated by appropriate cutoff filters in order to view and display its intensity on scale with the Raman scattering intensity. The observed band positions in the Raman spectrum of the unshocked HMX (cf. Fig. 10) are in excellent agreement with cw laser Raman measurements on the beta-polymorph of this compound.[18] As in the case of PETN, Fig. 11 shows a fairly uniform attenuation of the Raman spectrum during detonation but little or no shift in the band positions. It is interesting that we do not observe a comparable

loss of scattered 532-nm light intensity at this point in the detonation. Additional measurements have shown that significant depletion of the scattered laser light does not occur until ~50 ns after the parent molecule Raman spectrum becomes so weak that it can no longer be distinguished from the background emission. Hence, the observed interval for Raman signal attenuation cannot be attributed to a greatly reduced surface area for scattering and is not likely due to transient absorption.

We note that the reproducible, monotonic attenuation of PETN Raman scattering intensity over a 100 ns interval is consistent with previously obtained experimental and theoretical global reaction times for high-density PETN as well as recent velocity-interferometric measurements of reaction duration in other explosives.[19-21] Reaction times inferred from these preliminary free-surface studies are clearly not directly applicable to an unperturbed detonation reaction zone since, in this configuration, a rarefaction is reflected back into the explosive when the detonation front reaches the HE/vacuum interface. We anticipate less ambiguous results with optimal impedance-matching at the interface, and experiments utilizing appropriate window materials are planned. As yet, we have not observed Raman signals from transient or product species. Such observations may require a substantially improved signal-to-noise ratio, and we are currently implementing several modifications to the experimental arrangement which promise to greatly enhance the sensitivity and discrimination against background emission.

IV. SUMMARY

We have described the application of fast-framing photography and two real-time spectroscopic techniques to the study of microscopic chemical and physical changes in detonating HEs. Time-resolved emission spectroscopic results are consistent with early formation of $NO_2(A)$ followed by formation of other electronically excited radical products. High-resolution spectroscopy may be used to determine temperatures in the region of the detonation front. We have shown that quantitative single-pulse Raman scattering measurements can be made at the free surface of a detonating heterogeneous explosive and may provide a direct measure of reaction times in a detonation front. Refinement and further application of these techniques to experiments with well-characterized detonation fronts should provide valuable input for reactive flow models of detonation waves in heterogeneous explosives and lead to an improved predictive modelling capability of explosive initiation and performance.

ACKNOWLEDGEMENTS We wish to acknowledge the excellent technical assistance of H. C. Richardson and J. C. Pabst. We also thank S. A. Sheffield and M. E. Riley for helpful discussions.

References:

1. W. M. Trott and A. M. Renlund, "Single-pulse Raman scattering studies of heterogeneous explosive materials," Applied Optics, in press.

2. W. M. Trott, A. M. Renlund and R. G. Jungst, "Single-pulse Raman and photoacoustic spectroscopy studies of triamino-trinitrobenzene (TATB) and related compounds," Proceedings, 1985 Southwest Conference on Optics, SPIE, in press.

3. J. H. Blackburn and L. B. Seely, Trans. Faraday Soc. 61, 537 (1965)

4. N. Lundborg, Ark. Fys. 25, 541 (1964)

5. G. Herzberg, Molecular Spectra and Molecular Structure III. Electronic Spectra and Electronic Structure of polyatomic Molecules (Van Nostrand, New York, 1966)

6. A. M. Renlund and W. M. Trott, "Spectra of visible emission from detonating PETN and PBX 9407," Sandia Report, SAND83-2168.

7. K. P. Huber and G. Herzberg, Molecular Spectra and Molecular Structure IV. Constants of Diatomic Molecules (Van Nostrand, New York, 1979)

8. S. N. Suchard, Spectroscopic Data Vol. 1 (IFI/Plenum, New York, 1975)

9. C. L. Mader, Numerical Modeling of Detonation (University of California Press, Berkeley, 1979)

10. S. C. Schmidt, D. S. Moore and J. W. Shaner, in Proceedings of the American Physical Society Topical Conference on Shock Waves in Condensed Matter (Santa Fe, NM, 1983) p. 293.

11. A. Delpuech and A. Menil, in Proceedings of the American Physical Society Topical Conference on Shock Waves in Condensed Matter (Santa Fe, NM, 1983) p. 309.

12. C. Schulz, B. Linares, J. Cherville and S. Poulard, in Proc. Symp. on Explosives and Pyrotechnics, 8th (Los Angeles, CA, 1974) AD-789, p. 49.

13. A. Delpuech, J. Cherville and C. Michaud, in Proceedings of the 7th Symposium on Detonation (Annapolis, MD, 1981) p. 65.

14. M. H. Tailleur and J. Cherville, Propellants, Expl. and Pyrotech. 7, 22 (1982)

15. W. G. Von Holle, in Proceedings of the American Physical Society Topical Conference on Shock Waves in Condensed Matter (Santa Fe, NM, 1983) p. 283.

16. M. W. Jenner, T. J. Sinclair and D. P. Wyndham, in Raman Spectroscopy, Linear and Nonlinear, J. Lascombe and P. V. Huong, eds. (Wiley, New York, 1982) p. 243.

17. F. R. Dollish, W. G. Fateley and F. F. Bentley, Characteristic Raman Frequencies of Organic Compounds (Wiley, New York, 1974) p. 43.

18. Z. Iqbal, S. Bulusu and J. R. Autera, J. Chem. Phys. 60, 221 (1974)

19. A. N. Dremin, S. D. Savrov, V. S. Trofimov and K. K. Shvedov, Detonation Waves in Condensed Media, edited translation, AD-751 417, Wright-Patterson Air Force Base, Ohio, August 1972, p. 133.

20. E. L. Lee and C. M. Tarver, Phys. Fluids 23, 2362 (1980)

21. S. A. Sheffield, D. D. Bloomquist and C. M. Tarver, J. Chem. Phys. 80, 3831 (1984)

FIGURE CAPTIONS:

1. Schematic drawing of experimental arrangement for single-pulse Raman measurements.

2. Fast-framing photograph of detonating HNS. To illustrate the size of the image, the top trace is a record of the strobe-flash illuminated pellet.

3. Spectrum of emission from detonating HNS (ρ_o=1.7 g cm^{-3}) acquired over a 30-ns interval just prior to the break-out of the detonation front onto the face of the pellet (see text). The lines represent graybody curves at the temperatures shown, normalized to the observed emission intensity at 440 nm.

4. Spectrum of emission from detonating HNS (ρ_o=1.7 g cm^{-3}) acquired over a 30-ns interval during the peak of the emission intensity (see text).

5. Spectrum of emission from detonating HNS (ρ_o=1.7 g cm^{-3}) acquired over a 30-ns interval during the fall-off of the emission.

6. Time-integrated spectrum of CN(B-X) emission observed from detonating HNS (ρ_o=1.70 g cm^{-3}). The spectrum is corrected for the wavelength-dependent response of the spectrometer and detection system. The open circles are results from a computer-simulated spectrum with CN(B) rotational and vibrational temperatures of 5000 K.

7. Time-integrated spectrum of CN(B-X) emission observed from detonating HNS (ρ_o=1.50 g cm^{-3}). The spectrum is corrected for the wavelength-dependent response of the spectrometer and detection system. The open circles are results from a computer-simulated spectrum with CN(B) rotational and vibrational temperatures of 6500 K.

8. Single-pulse Raman spectra from unshocked PETN and a detonating sample as recorded by the optical multichannel analyzer (100-ns gate width). Broadband emission from the detonation is evident on the top trace.

9. Temporal profiles of Raman signal intensity and emission intensity from detonating. PETN. Each open circle represents a single-shot measurement of the 1296 cm^{-1} Raman signal intensity at the indicated time delay divided by the signal intensity from the unshocked material. Raman signal intensities from the unshocked material were reproducible to within a few percent.

10. Single-pulse Raman spectrum from unshocked HMX. The scattered 532-nm laser light is also displayed.

11. Single-pulse Raman spectrum from detonating HMX acquired ~50 ns after arrival of the detonation front to the front surface of the pellet. Broadband emission from the detonation contributes to the high background level. The Raman signal intensities are considerably reduced from the previous figure, but the scattered 532-nm laser light remains unaffected at this delay time.

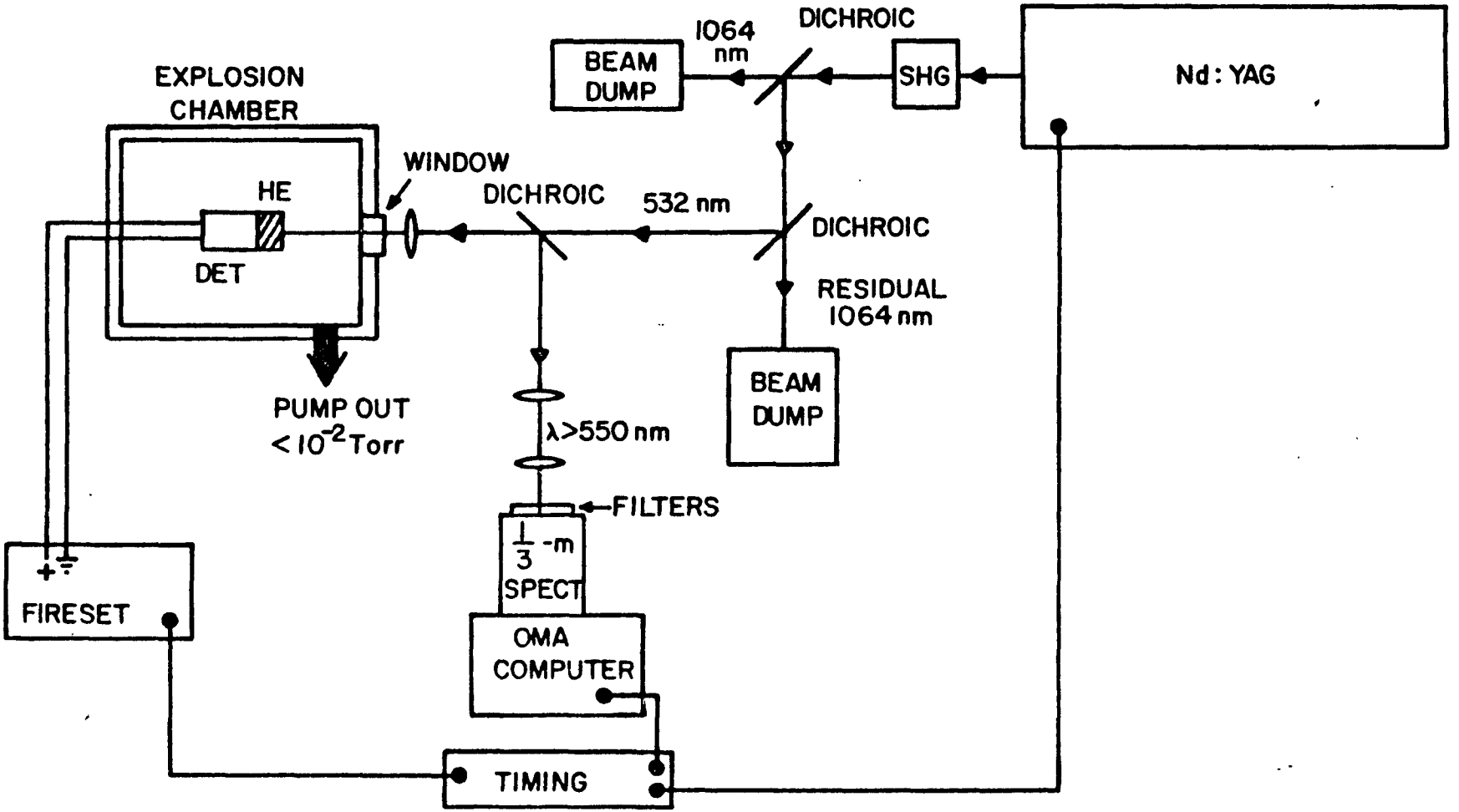
EXPLOSION CHAMBER
HE
DET
WINDOW
DICHROIC
532 nm
DICHROIC
1064 nm
DICHROIC
BEAM DUMP
SHG
Nd : YAG
RESIDUAL 1064 nm
BEAM DUMP
PUMP OUT
< 10^-2 Torr
λ>550 nm
FILTERS
1/3 -m SPECT
OMA COMPUTER
FIRESET
TIMING

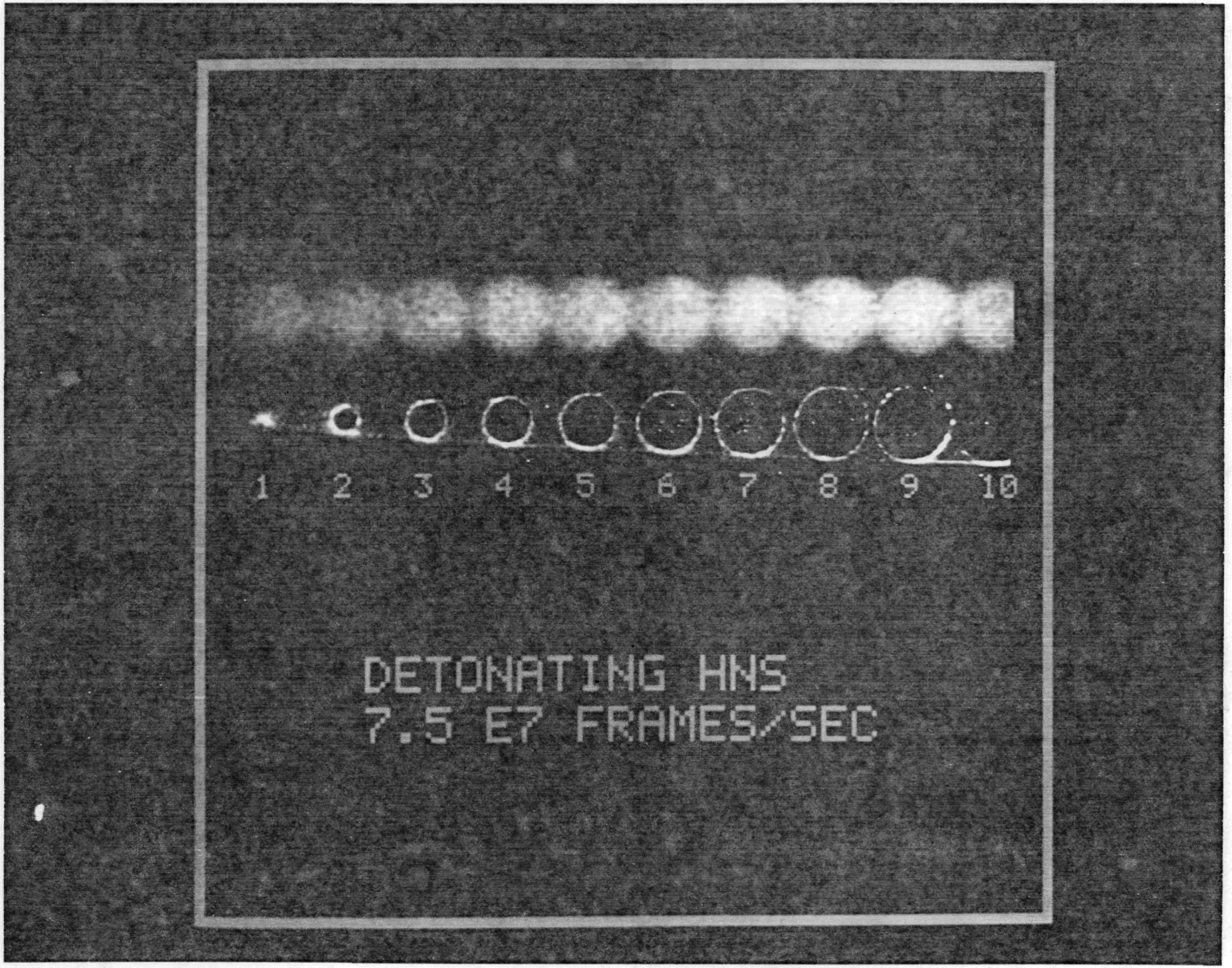

Fig. 2

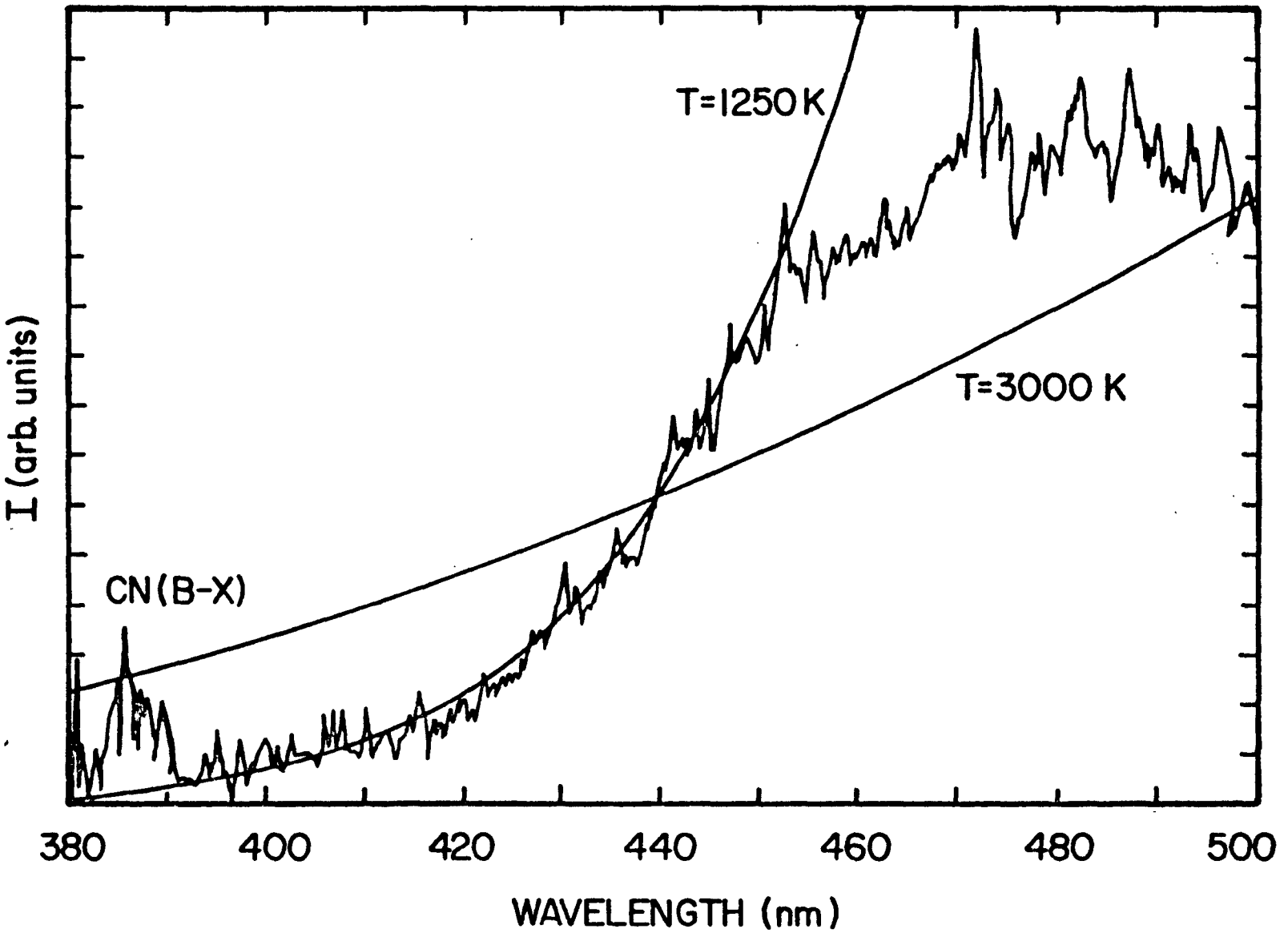
T=1250 K
T=3000 K
CN(B-X)
I (arb. units)
380
400
420
440
460
480
500
WAVELENGTH (nm)

Fig. 3

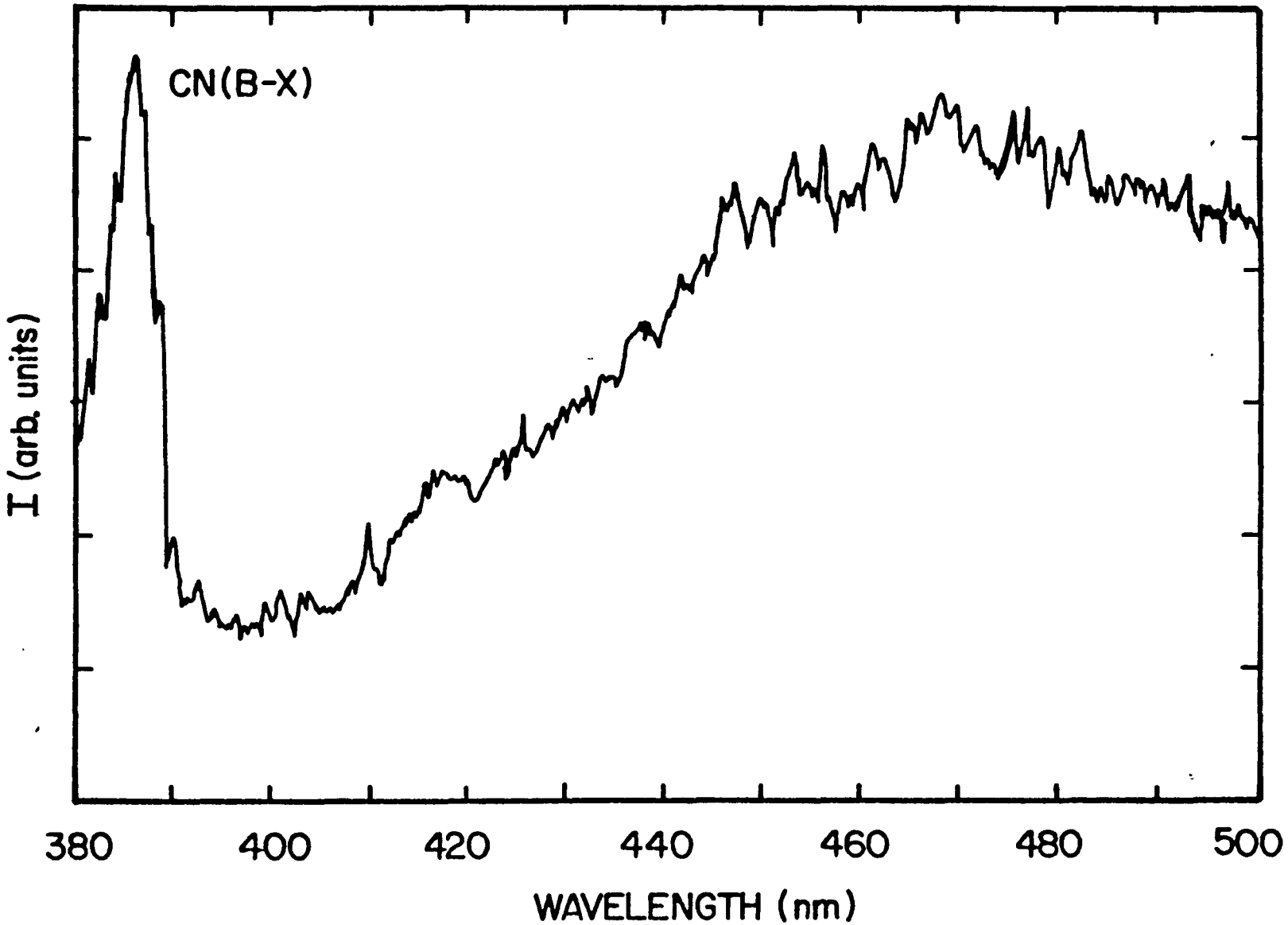

Fig 4

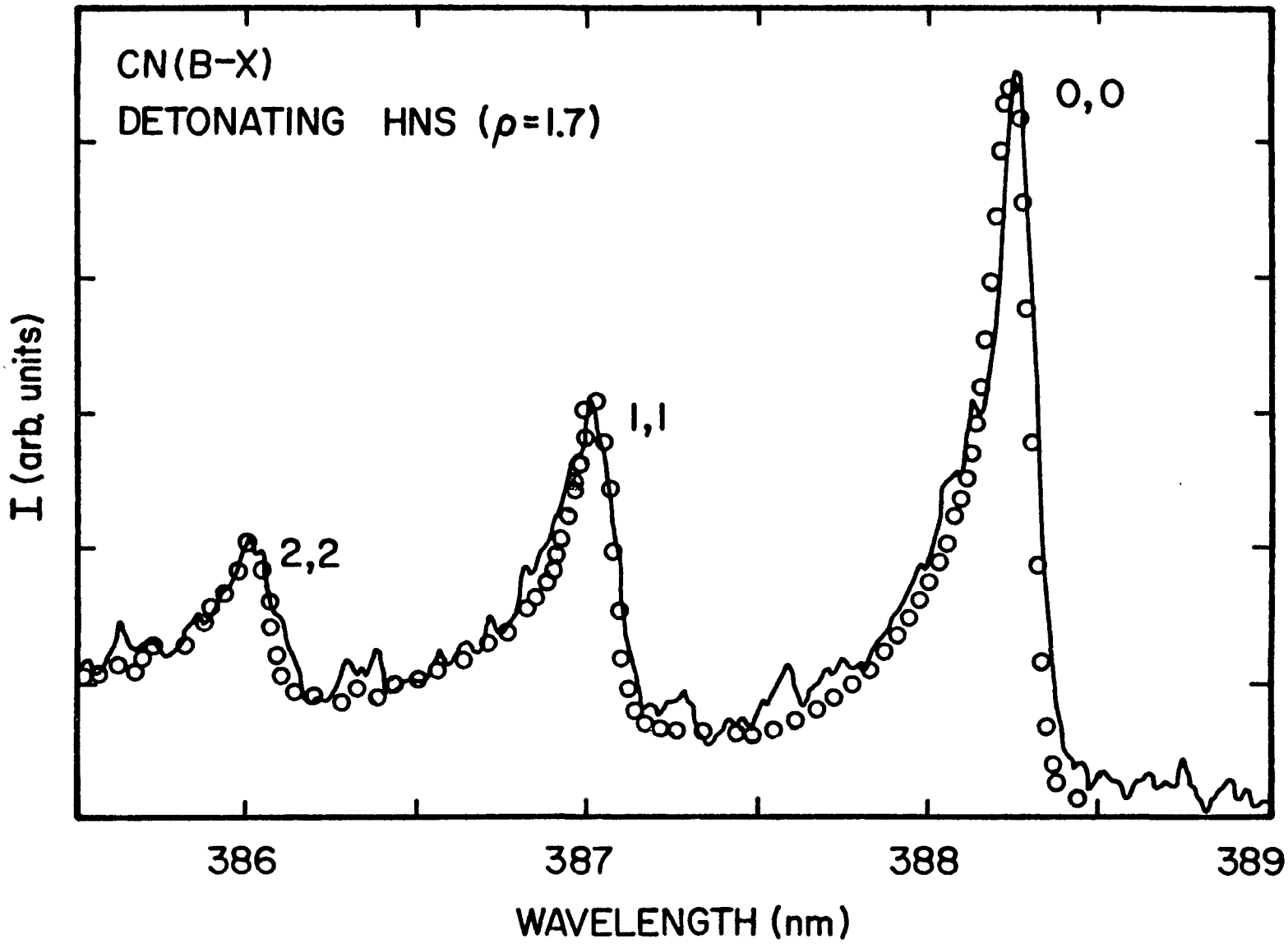
CN(B-X)
DETONATING HNS (ρ=1.7)
0,0
1,1
2,2
I (arb. units)
386
387
388
389
WAVELENGTH (nm)

Fig 1

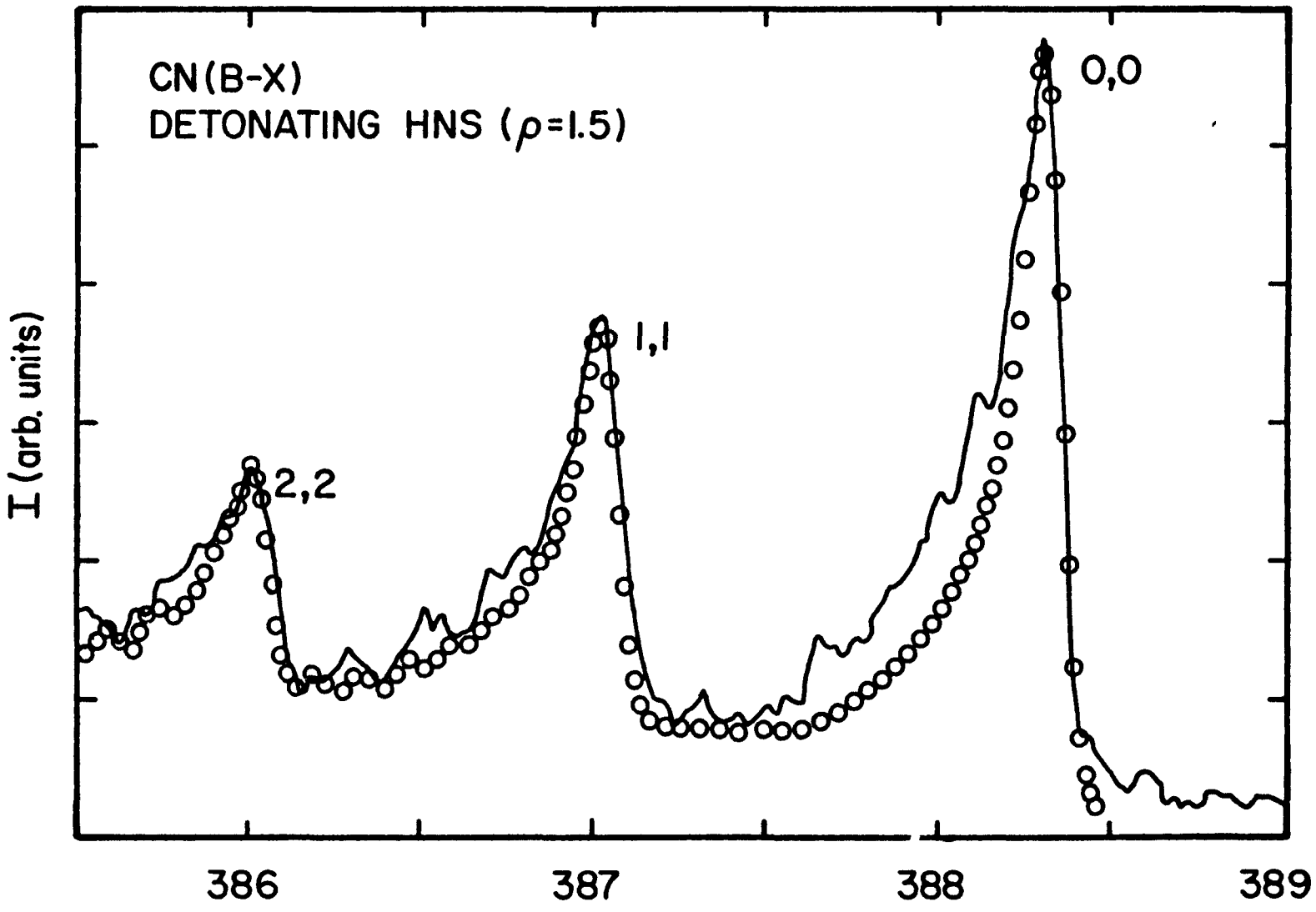
CN(B-X)
DETONATING HNS (ρ=1.5)
0,0
1,1
2,2
I (arb. units)
386
387
388
389

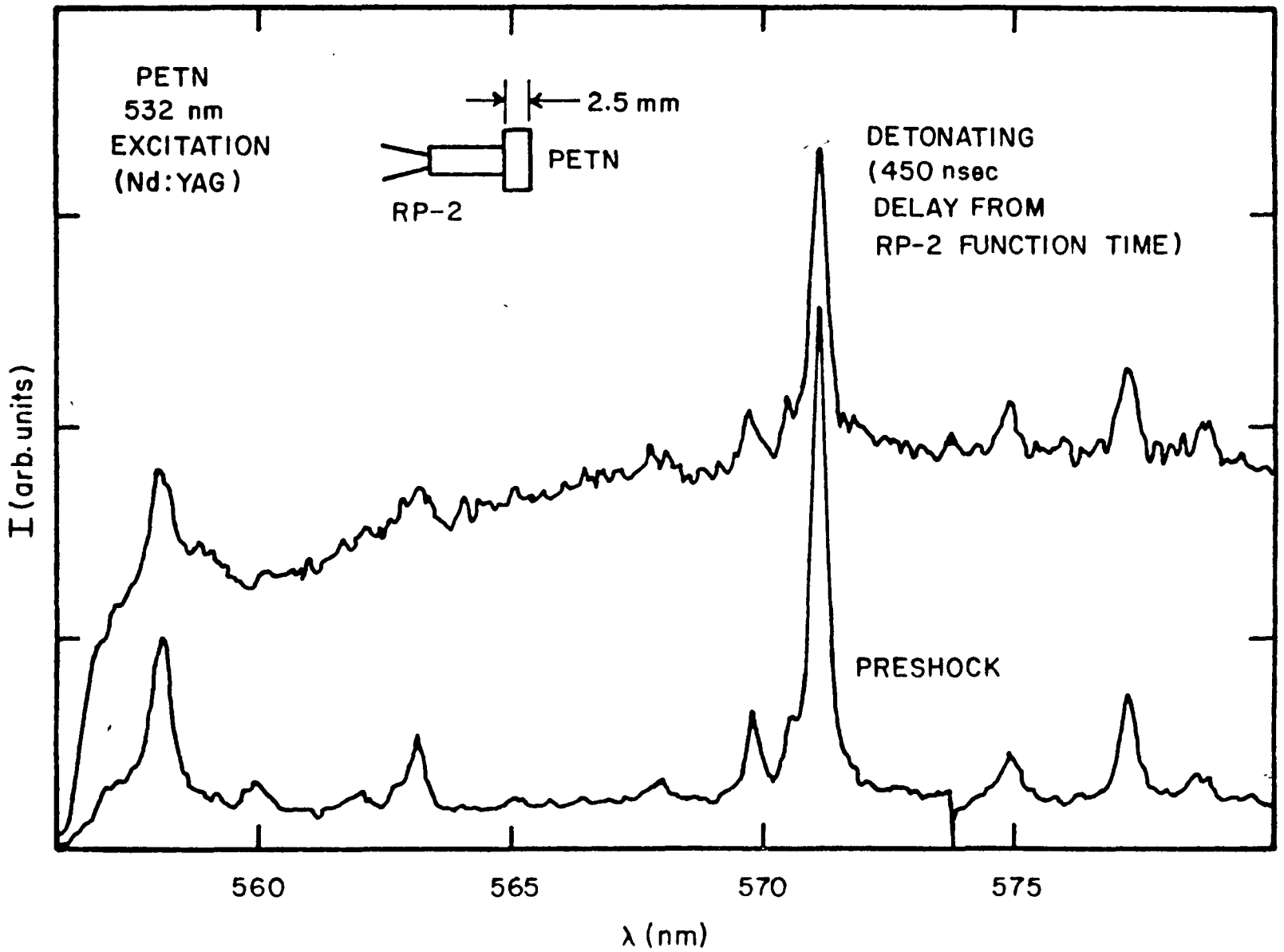
PETN
532 nm
EXCITATION
(Nd:YAG)
2.5 mm
PETN
RP-2
DETONATING
(450 nsec
DELAY FROM
RP-2 FUNCTION TIME)
PRESHOCK
I (arb. units)
560
565
570
575
λ (nm)

Fig. 9

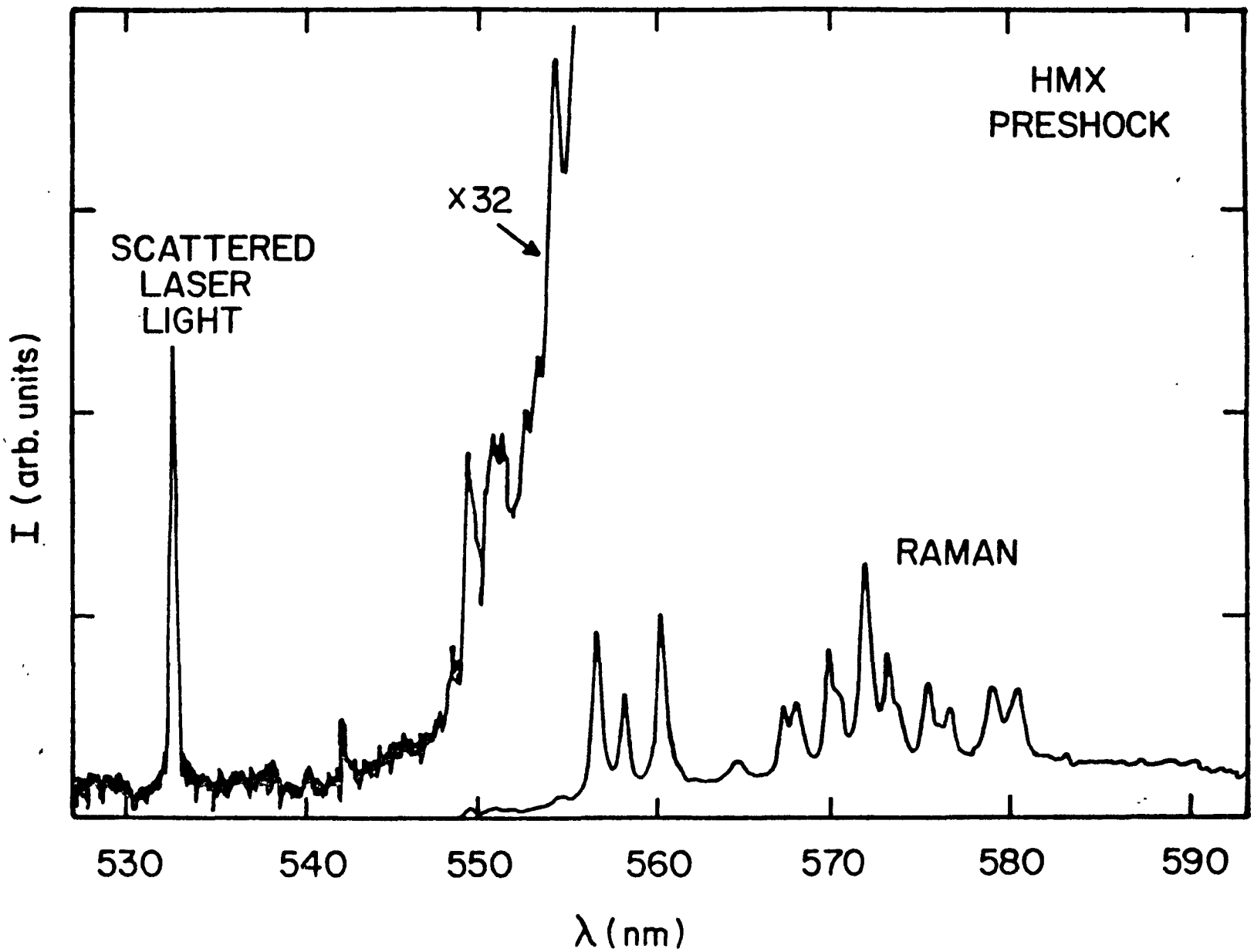
HMX
PRESHOCK
x32
SCATTERED
LASER
LIGHT
RAMAN
I (arb. units)
530
540
550
560
570
580
590
λ (nm)

Fig. 10

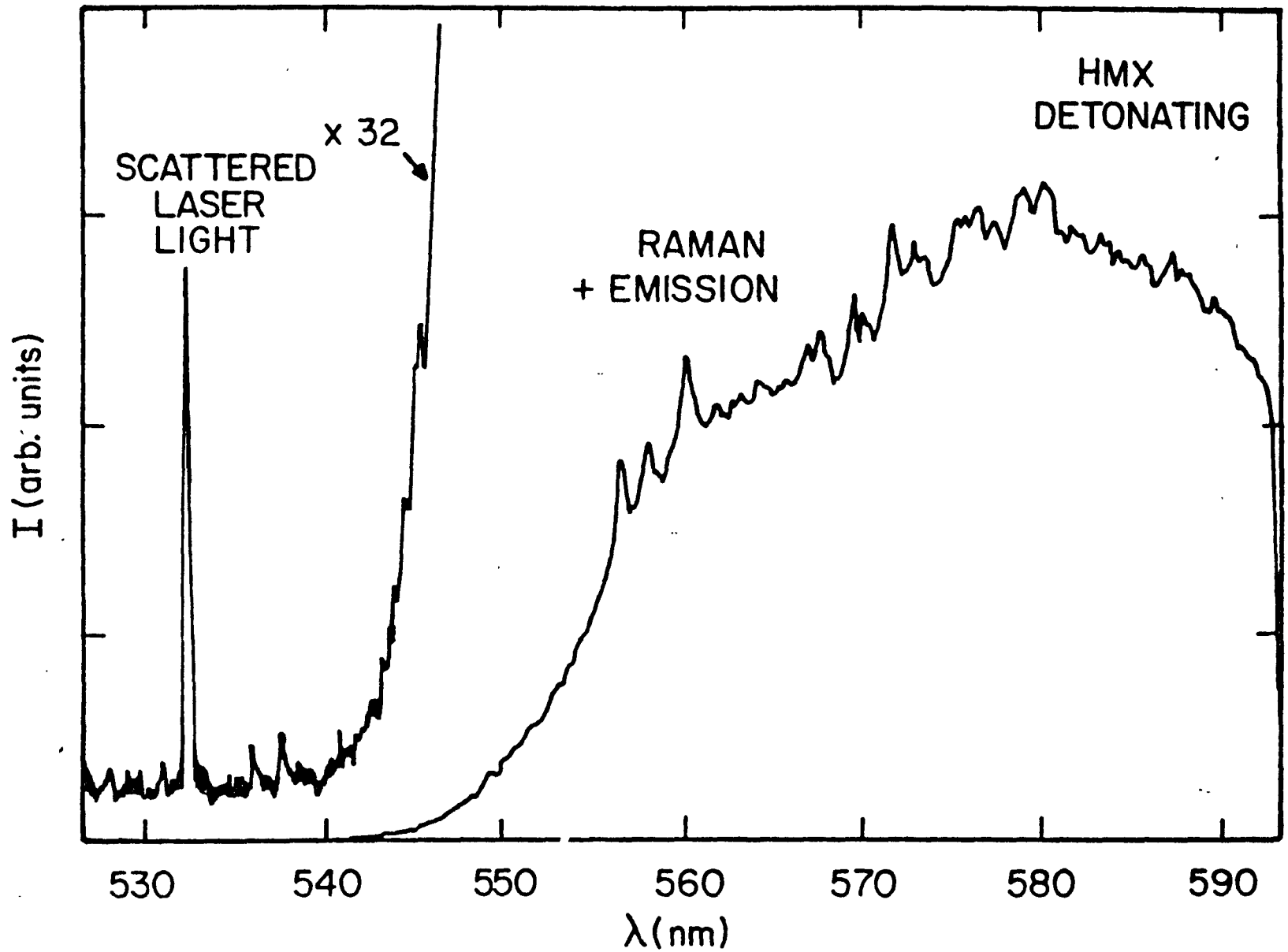
HMX
DETONATING
x 32
SCATTERED
LASER
LIGHT
RAMAN
+ EMISSION
I (arb. units)
530
540
550
560
570
580
590
λ(nm)

Fig. 11